JOURNAL OF SOLID STATE CHEMISTRY 3, 56–66 (1971)

Trigonal-Prismatic Coordination in Solid Compounds of Transition Metals

R. HUISMAN*, R. DE JONGE†, C. HAAS, AND F. JELLINEK

Laboratory of Inorganic Chemistry, Materials Science Center of the University, Bloemsingel 10, *Groningen, The Netherlands*

Received July 23, 1970

The ligand-field splitting of *d* levels in trigonal-prismatic coordination is discussed in terms of crystal-field and simple molecular-orbital calculations. It is found that *d*-covalency provides a stabilizing factor for trigonal-prismatic coordination, as compared with octahedral coordination, for atoms with d^0, d^1 or d^2 configuration. This effect qualitatively explains the occurrence of trigonal-prismatic coordination in strongly covalent 4*d* and 5*d* transition-metal chalcogenides, in which the metal atoms have d^1 or d^2 configuration. The same type of arguments are used to explain the stability of trigonal-prismatic coordination of alkali metals in some intercalation compounds. The stability of structures with trigonal-prismatic coordination of d^0 anions, such as the NiAs and MnP types, is also attributed to this effect. The physical properties of 4*d* and 5*d* transition-metal dichalcogenides are correlated with schematic energy-band diagrams, which are consistent with the ligand-field splitting of the *d* levels derived in earlier sections of this paper.

Introduction

Trigonal-prismatic coordination has received less attention than, for instance, octahedral or tetrahedral coordination. This is probably due to the fact that trigonal-prismatic coordination is rather unusual in isolated complexes. Only in a few cases trigonal-prismatic coordination has been established in coordination compounds, for instance in the complexes $Mo(S_2C_2H_2)_3$ (*1*), $Re(S_2C_2Ph_2)_3$ (*2*), and $V(S_2C_2Ph_2)_3$ (*3*). Probably, it is also present in several other tris(1,2-dithiolato) complexes of V, Cr, Mo, W, and Re (*4*, *5*).

However, trigonal-prismatic coordination is far more common in solid compounds of transition metals, as is shown by the following examples:

(1) The disulfides (*6*) and diselenides (*7*) of Nb, Ta, Mo, and W, and α-$MoTe_2$ (*7*) have layer structures with trigonal-prismatic coordination of the metal atoms. The iodide β-ThI_2 has a layer structure with half of the metal atoms in trigonal-prismatic, and half in octahedral coordination (*8*).

(2) Additional metal atoms may be intercalated between the layers of NbX_2 and TaX_2 (X = S, Se), leading to phases of compositions $Nb_{1+p}X_2$ and $Ta_{1+p}X_2$ (generally with $0 < p < 0.3$), (*6*, *9*); Cu_pNbX_2, Cu_pTaS_2, Ag_pNbS_2, Ag_pTaS_2 (with $p \approx \frac{2}{3}$), (*10*, *11*); T_pNbX_2 and T_pTaX_2 (T = 3*d* transition metal; $p = \frac{1}{3}$ or $\frac{1}{4}$), (*12–16*). In all these compounds the coordination of Nb and Ta (within the layers) is trigonal-prismatic. The corresponding intercalation compounds of Mo and W have not been found.

(3) Intercalation compounds A_pMoS_2 and A_pWS_2 (A = alkali metal; $p \approx \frac{1}{2}$) exist, but these compounds are highly reactive and thermally unstable (*17*). This is in marked contrast with the compounds A_pNbX_2 and A_pTaX_2 (A = Na, K; $p \approx \frac{2}{3}$) which are quite stable; again, Nb and Ta have trigonal-prismatic coordination (*18*).

(4) As a result of the structure of the NbX_2 or TaX_2 layers in the compounds A_pNbX_2 and A_pTaX_2, the environment of the intercalated alkali metals A can be either octahedral, trigonal-prismatic or tetrahedral. For X = Se trigonal-prismatic coordination of the alkali metals was found,

* Present address, AKZO Research and Engineering N.V., Arnhem, The Netherlands.

† Present address, Central Laboratory DSM, Geleen, The Netherlands.

for X = S both octahedral and trigonal-prismatic coordination occur (*18*). In the related intercalation compounds A_pTiS_2 (A = Li, Na, K, Cs; $p = 0.8$–0.5) the alkali metals Li and Na have octahedral, K and Cs trigonal-prismatic coordination; the environment of Ti is octahedral in all cases (*19*). (The $NaCrS_2$-type structure recently reported for $KTiS_2$ (*20*) is incorrect.) The compounds $A_2Pt_4S_6$ (A = K, Rb, Cs) and isotypes also have layer structures with the alkali metals intercalated between trigonal layers $S_3Pt_4S_3$; again the coordination of K, Rb and Cs is trigonal-prismatic (*21*).

(5) Both metal and nonmetal atoms have trigonal-prismatic coordination in NbP, TaP, NbAs and TaAs, which have structures of the NbAs type (*7*). The same is true of phases with WC-type structures, such as MoP (*22*), ZrS_{1-x} (*6*), $ZrSe_{1-x}$, $ZrTe_{1-x}$ (*23*), HfS (*24*), HfSe (*25*), and possibly TiS_{1-x} (*6*).

(6) Trigonal-prismatic coordination of anions is also found in several other structure types, the most common being the NiAs type and its derivatives (*26*), such as the MnP type. Structures of these types are known for many sulfides, selenides, tellurides, phosphides, arsenides and antimonides of transition metals (*7*), but not for oxides or nitrides.

These examples show that trigonal-prismatic coordination is more common for 4*d* and 5*d* transition-metal atoms than for 3*d* metal atoms (see examples 1, 2, 3, and 5). In nearly all cases the metal atoms with trigonal-prismatic coordination have a formal configuration d^1 or d^2 (exceptions are MoP and some nitrides and carbides of the WC type). The alkali metals K, Rb, and Cs in the compounds mentioned under (4) have the configuration $s^2p^6d^0$, or, briefly, d^0; the same applies to the anions with trigonal-prismatic coordination, mentioned in examples 5, 6 (again, nitrides and carbides of the WC type are exceptions).

In some compounds trigonal-prismatic coordination is found at low temperatures, octahedral coordination at high temperatures. This is the case for the d^0 anions in MnSe and MnTe, which compounds transform from the NiAs type to the NaCl type at −13°C (*27*) and 1050°C (*28*), respectively. In $TaSe_2$, the coordination of the d^1 cation is trigonal-prismatic below 790°C and octahedral above 860°C, whereas at intermediate temperatures the two types of coordination coexist within one phase (*29*). Similar transitions (at somewhat higher temperatures) are found in $NbSe_2$ (*30*). The transition of $MoTe_2$ at about 850°C, leading from trigonal-prismatic to (distorted) octahedral coordination of the d^2 cation, is accompanied by a change from semiconducting to metallic properties (*31*).

These transitions clearly demonstrate that trigonal-prismatic coordination has the lower energy, octahedral coordination the higher entropy in the compounds concerned. In $TaSe_2$ the difference in energy between the two types of coordination is about 4 kcal/mol, the difference in entropy about 4 cal/mol·deg (*32*); for $NbSe_2$ somewhat lower values were found (*30*).

In this paper several problems related to trigonal-prismatic coordination of atoms are discussed. The first question is why this type of coordination is stable with respect to the more common octahedral coordination, and in particular, why this is apparently so only for atoms with configurations d^0, d^1, and d^2. Electrostatic considerations of Madelung energy and Born repulsion show in all cases a larger stability for octahedral coordination (*33*). However, using simple molecular-orbital considerations, it will be shown that *d*-covalency has a stabilizing effect on trigonal-prismatic coordination of atoms with d^0, d^1, or d^2 configuration.

There is difference of opinion in the literature about the ligand-field splitting of *d* levels for trigonal-prismatic coordination. Some authors (*34*, *35*) assume the degenerate level e'^*, others (*7*, *16*, *36*) the nondegenerate level $a_1'^*$ to have the lowest energy. Evidence presented in this paper, strongly favours $a_1'^*$ as the lowest energy level of *d* electrons in trigonal-prismatic coordination.

The order of the *d* levels has repercussions for the interpretation of the electrical, magnetic, and optical properties of the dichalcogenides of Nb, Ta, Mo, and W. In a final section, available experimental data [an extensive review was recently published by Wilson and Yoffe (*37*)] are discussed in terms of simple band-structure models.

Crystal-Field Splitting of d Levels

The simplest way to account for the splitting of the *d* levels is by a crystal-field calculation. In calculations of this type, the ligand atoms surrounding the central atom are replaced by point charges *Ze*. The electrostatic potential *V*, caused by these charges, can be expanded in a series of spherical

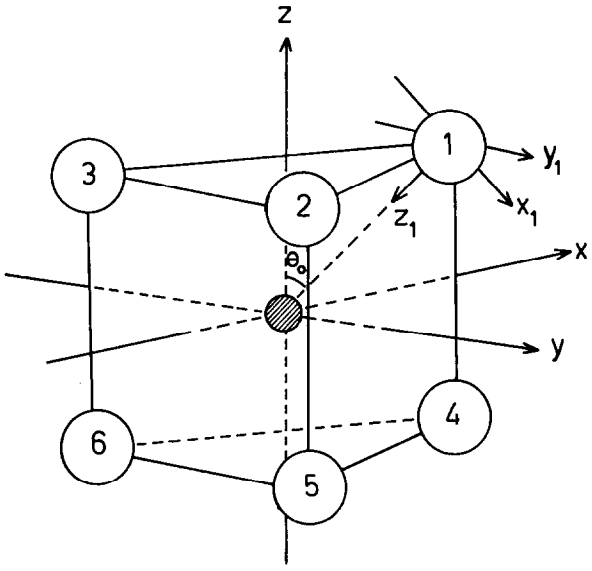

FIG. 1. Trigonal-prismatic coordination; coordinate systems used in molecular-orbital calculations.

harmonics $Y_l^m(\theta,\phi)$. For a trigonal prism (Fig. 1), one obtains (*34*, *38*)

$$\text{eV} = 7\left(\frac{4\pi}{5}\right)^{1/2} Ar^2\, Y_2^0(\theta,\phi) + 7(4\pi)^{1/2} Br^4\, Y_4^0(\theta,\phi), \quad (1)$$

with

$$A = (\tfrac{3}{7})(3\cos^2\theta_0 - 1)\left(\frac{e^2 Z}{R^3}\right)$$

and

$$B = (\tfrac{1}{28})(35\cos^4\theta_0 - 30\cos^2\theta_0 + 3)\left(\frac{e^2 Z}{R^5}\right).$$

In the above equations R is the metal–ligand distance, and θ_0 is the angle between the trigonal axis and the line connecting central and ligand atoms, see Fig. 1.

The d-electron wavefunctions of the central atom can be written as $R(r)\, Y_l^m(\theta,\phi)$. The energy levels E_m are the diagonal matrix elements of eV, and are given by

$$\begin{aligned} E_0 &= 2A\overline{r^2} + 6B\overline{r^4}, \\ E_{\pm 1} &= A\overline{r^2} - 4B\overline{r^4}, \\ E_{\pm 2} &= -2A\overline{r^2} + B\overline{r^4}, \end{aligned} \quad (2)$$

with

$$\overline{r^k} = \int_0^\infty |R(r)|^2 r^{k+2}\, dr.$$

For all reasonable values of θ_0 and $\overline{r^2}/\overline{r^4}$, the $m = \pm 1$ level has the highest energy. However, whether the $m = 0$ or the $m = \pm 2$ level has the lowest energy, depends in a rather sensitive way on the values of θ_0 and $\overline{r^2}/\overline{r^4}$.

The values of θ_0 observed in compounds of the MoS_2 type, are close to the value $\theta_0 = 49°6'$ (or $\cos^2\theta = \frac{3}{7}$) for an ideal prism (with all edges equal). Values of $\overline{r^2}/\overline{r^4}$ can be calculated if the radial part of the wavefunction is known. Using simple Slater functions (*39*), one finds that the $m = 0$ and $m = \pm 2$ levels lie close to each other for compounds of the MoS_2 type. However, the use of better wavefunctions [we employed the analytical approximations to the numerical Hartree–Fock wavefunctions according to Basch and Gray (*40*)] leads to an appreciable splitting, with the $m = \pm 2$ level (e') as the lowest energy level.

This result is at variance with the interpretation of the physical properties of MoS_2-type compounds, to be presented later. Generally, however, crystal-field calculations are not expected to give a reliable description of the ligand-field splitting. A molecular-orbital calculation, indicating that the $m = 0$ (a_1') level has the lowest energy, is given in the following section.

Qualitative Molecular-Orbital Calculations

In this section a simple qualitative molecular-orbital calculation of the Hückel type is given for trigonal-prismatic and octahedral coordination. In first instance, only metal d orbitals and ligand p orbitals are considered. The metal d orbitals are expressed in a coordinate system, centered on the metal atom, with z parallel to the trigonal axis (Fig. 1). For each ligand i a coordinate system is chosen with z_i pointing in the direction of the metal, and x_i in the $z - z_i$ plane (Fig. 1). The ligand p orbitals are σ_i (p orbital along z_i axis), π_{vi} (along x_i) and π_{hi} (along y_i). The σ_i orbitals are responsible for σ, the π_{vi} and π_{hi} orbitals for π-bonding. The orbitals can be classified according to the irreducible representations of the symmetry group D_{3h} of the trigonal prism. The result for d and σ orbitals is given in Table I.

First, all overlap integrals are neglected, and only σ-bonding is taken into account. The energy levels then depend only on the angle θ_0, on the energy difference Δ between d and σ orbitals, and on the overlap energy V_σ, defined as $V_\sigma = \int \phi_d{}^i H \sigma_i\, dv$, where $\phi_d{}^i$ is a metal d function constructed in such a way that it has maximum overlap with the σ_i orbital of ligand i, see Fig. 2.

In order to carry out the calculations, the orbitals $\phi_d{}^m(r,\theta,\phi)$ are transformed into new orbitals

TABLE I

d AND σ ORBITALS IN A TRIGONAL PRISM [$\epsilon = \exp(2\pi i/3)$; $\epsilon^* = \exp(-2\pi i/3)$]

	Metal, ϕ_d^m	Ligand functions, ϕ_L^m	V_σ^m
A_1'	ϕ_d^0	$6^{-1/2}(\sigma_1 + \sigma_2 + \sigma_3 + \sigma_4 + \sigma_5 + \sigma_6)$	$(\frac{3}{2})^{1/2}(3\cos^2\theta_0 - 1)\,V_\sigma$
A_2''	—	$6^{-1/2}(\sigma_1 + \sigma_2 + \sigma_3 - \sigma_4 - \sigma_5 - \sigma_6)$	Nonbonding
E'	$\left\{\begin{matrix}\phi_d^2 \\ \phi_d^{-2}\end{matrix}\right.$	$\left.\begin{matrix}6^{-1/2}(\sigma_1 + \epsilon\sigma_2 + \epsilon^*\sigma_3 + \sigma_4 + \epsilon\sigma_5 + \epsilon^*\sigma_6) \\ 6^{-1/2}(\sigma_1 + \epsilon^*\sigma_2 + \epsilon\sigma_3 + \sigma_4 + \epsilon^*\sigma_5 + \epsilon\sigma_6)\end{matrix}\right\}$	$\frac{3}{2}\sin^2\theta_0\,V_\sigma$
E''	$\left\{\begin{matrix}\phi_d^1 \\ \phi_d^{-1}\end{matrix}\right.$	$\left.\begin{matrix}6^{-1/2}(\sigma_1 + \epsilon^*\sigma_2 + \epsilon\sigma_3 - \sigma_4 - \epsilon^*\sigma_5 - \epsilon\sigma_6) \\ 6^{-1/2}(\sigma_1 + \epsilon\sigma_2 + \epsilon^*\sigma_3 - \sigma_4 - \epsilon\sigma_5 - \epsilon^*\sigma_6)\end{matrix}\right\}$	$3\sin\theta_0\cos\theta_0\,V_\sigma$

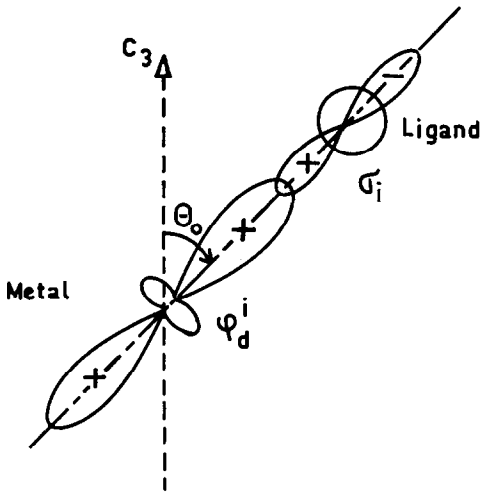

FIG. 2. Overlap between metal d orbital and ligand σ function.

$\phi_d^{m'}(r, \theta_i, \phi_i)$, which are functions of the polar coordinates θ_i, ϕ_i of a coordinate system with axes parallel to $x_i\,y_i\,z_i$:

$$\phi_d^m(r, \theta, \phi) = \sum_{m'} A_{mm'}(\theta_{0i}, \phi_{0i})\,\phi_d^{m'}(r, \theta_i, \phi_i). \quad (3)$$

The transformation coefficients $A_{mm'}$ depend on the coordinates θ_{0i}, ϕ_{0i} of ligand i. The ligands are numbered as shown in Fig. 1. For these ligand positions

$$\theta_{01} = \theta_{02} = \theta_{03} = \theta_0, \quad \theta_{04} = \theta_{05} = \theta_{06} = 180° - \theta_0,$$
$$\phi_{01} = \phi_{04} = 0, \quad \phi_{02} = \phi_{05} = 120°, \quad \phi_{03} = \phi_{06} = 240°.$$

The coefficients A_{mo} are given by

$$A_{mo} = \left(\frac{4\pi}{5}\right)^{1/2} Y_2^m(\theta_{0i}, \phi_{0i}). \quad (4)$$

The overlap energy V_σ^m of ϕ_d^m with a ligand function

$$\phi_L = \sum_i a_i\,\sigma_i$$

is given by

$$V_\sigma^m = \int \phi_d^m\,H\phi_L\,dv = \sum_i a_i \int \phi_d^m\,H\sigma_i\,dv. \quad (5)$$

Substitution of Eqs. (3) and (4) gives

$$V_\sigma^m = \sum_i a_i \left(\frac{4\pi}{5}\right)^{1/2} V_\sigma\,Y_2^m(\theta_{0i}, \phi_{0i}). \quad (6)$$

From this equation the matrix elements V_σ^m are easily obtained; the results are included in Table I. As each d function has a nonvanishing matrix element with only one ligand function, the eigenvalues of the energy are given by

$$E^m = -\tfrac{1}{2}\Delta \pm \tfrac{1}{2}\{\Delta^2 + 4(V_\sigma^m)^2\}^{1/2}. \quad (7)$$

The results are given in Table II.

By rotating one triangle of ligand atoms over an angle of 60°, the trigonal prism is transformed into a trigonally distorted octahedron (symmetry D_{3d}). The energy levels for this coordination can be expressed in the same way in terms of the overlap energy V_σ. The results are given in Table III. For an

TABLE II

ENERGY LEVELS FOR A TRIGONAL PRISM (σ-BONDING ONLY; ANTIBONDING AND NONBONDING LEVELS ARE INDICATED BY AN ASTERISK AND BY nb, RESPECTIVELY)

$$E(e''^*) = \tfrac{1}{2}\Delta[-1 + (1 + \alpha_3)^{1/2}]$$
$$E(e'^*) = \tfrac{1}{2}\Delta[-1 + (1 + \alpha_2)^{1/2}]$$
$$E(a_1'^*) = \tfrac{1}{2}\Delta[-1 + (1 + \alpha_1)^{1/2}]$$
$$E(a_2'')_{nb} = -\Delta$$
$$E(a_1') = \tfrac{1}{2}\Delta[-1 - (1 + \alpha_1)^{1/2}]$$
$$E(e') = \tfrac{1}{2}\Delta[-1 - (1 + \alpha_2)^{1/2}]$$
$$E(e'') = \tfrac{1}{2}\Delta[-1 - (1 + \alpha_3)^{1/2}]$$

with

$$\alpha_1 = 6(V_\sigma/\Delta)^2(3\cos^2\theta_0 - 1)^2$$
$$\alpha_2 = 9(V_\sigma/\Delta)^2\sin^4\theta_0$$
$$\alpha_3 = 36(V_\sigma/\Delta)^2\sin^2\theta_0\cos^2\theta_0$$

TABLE III

ENERGY LEVELS FOR A TRIGONALLY DISTORTED OCTAHEDRON (TRIGONAL ANTIPRISM); σ-BONDING ONLY. THE EQUATIONS FOR α_1, α_2, AND α_3 ARE GIVEN IN TABLE II

$$E(e_g^*) = \tfrac{1}{2}\Delta[-1 + (1 + \alpha_2 + \alpha_3)^{1/2}]$$
$$E(a_{1g}^*) = \tfrac{1}{2}\Delta[-1 + (1 + \alpha_1)^{1/2}]$$
$$E(e_g)_{nb} = 0$$
$$E(a_{2u})_{nb} = -\Delta$$
$$E(e_u)_{nb} = -\Delta$$
$$E(a_{1g}) = \tfrac{1}{2}\Delta[-1 - (1 + \alpha_1)^{1/2}]$$
$$E(e_g) = \tfrac{1}{2}\Delta[-1 - (1 + \alpha_2 + \alpha_3)^{1/2}]$$

ideal octahedron ($\cos^2\theta_0 = \frac{1}{3}$; symmetry O_h) the a_{1g} and e_g levels coalesce into the t_{2g} level. In Fig. 3, the energy levels for an ideal trigonal prism ($\cos^2\theta_0 = \frac{3}{7}$) and an ideal octahedron ($\cos^2\theta_0 = \frac{1}{3}$) are compared.

The effect of π-bonding was also investigated.[1] The contributions of π-bonding can be expressed in terms of an overlap energy

$$V_\pi = \int \phi_d^{i,\pm 1} H \pi^{i,\pm 1}\, dv,$$

[1] Details of these calculations are given in Ref. *32*.

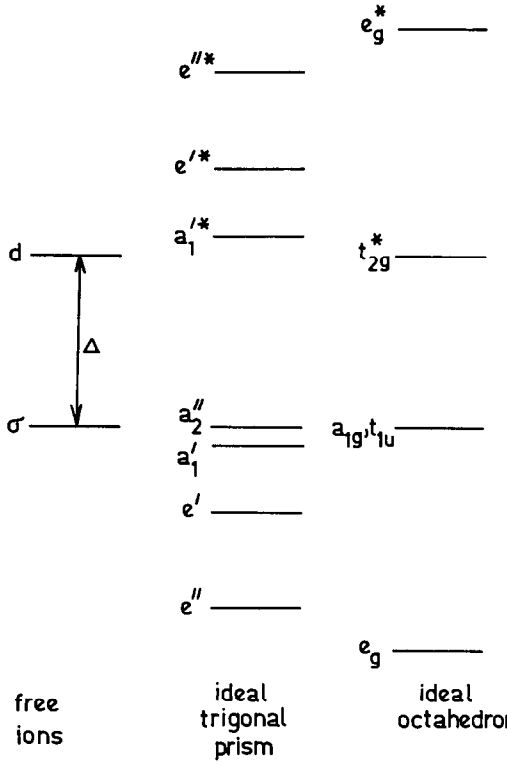

FIG. 3. Energy levels for an ideal trigonal prism ($\cos^2\theta_0 = \frac{3}{7}$) and an ideal octahedron ($\cos^2\theta_0 = \frac{1}{3}$) for $V_\sigma/\Delta = 1$; only σ-bonding is taken into account.

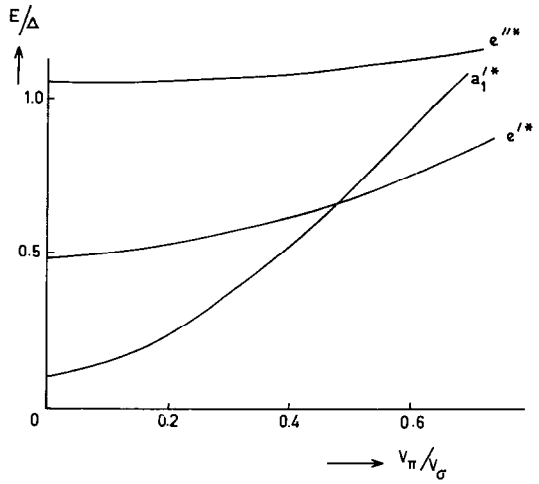

FIG. 4. Ligand-field splitting of d levels for ideal trigonal-prismatic coordination as a function of increasing π-bonding (the curves are for the case $V_\sigma = \Delta$).

where $\phi_d^{i,\pm 1}$ and $\pi^{i,\pm 1}$ are d orbitals of the central atom and p orbitals of ligand i, respectively, with magnetic quantum numbers $m' = \pm 1$ with respect to the metal–ligand i direction. The result of these calculations is given in Fig. 4. For σ-bonding only, the $a_1'^*$ level is the antibonding level with the lowest energy. Increasing π-bonding, however, decreases the energy difference between the $a_1'^*$ and e'^* levels.

Semiempirical Calculations for MoS_2

Semiempirical calculations of the Hückel type were carried out for the ligand-field splitting of d levels in MoS_2. Analytical approximations to the numerical Hartree–Fock wavefunctions, given by Basch and Gray (*40*), were used for the radial $4d$ functions of Mo. For the $3s$ and $3p$ valence orbitals of sulfur SCF functions tabulated by Clementi (*41*) were used. The overlap integrals calculated with these functions for a Mo–S distance of 2.409 Å are $S(4d_\sigma - 3s) = 0.140$, $S(4d_\sigma - 3p_\sigma) = 0.153$, and $S(4d_\pi - 3p_\pi) = 0.112$. The $4d_\sigma$ and $4d_\pi$ orbitals are d orbitals with orbital quantum numbers $m' = 0$ and $m' = \pm 1$ with respect to the metal–ligand axis. From these S values the group overlap integrals were calculated (*42*, *32*); the results are given in Table IV.

For the Coulomb integrals, the negative values of the valence-state ionization energies (VSIE) were used. In order to take account of the electronic repulsion, a procedure proposed by Viste and Gray (*43*) was followed. The spectroscopic data from which VSIE values are obtained, have been given

TABLE IV

GROUP OVERLAP INTEGRALS FOR A MoS_6 TRIGONAL PRISM WITH $\theta_0 = 49°6'$ AND $R = 2.409$ Å

$G(a_1')\,\sigma_s = 0.049$	
$G(a_1')\,\sigma_p = 0.054$	
$G(a_1')\,\pi_v = -0.235$	
$G(e')\,\sigma_s = 0.120$	$G(e'')\,\sigma_s = 0.208$
$G(e')\,\sigma_p = 0.131$	$G(e'')\,\sigma_p = 0.227$
$G(e')\,\pi_v = 0.096$	$G(e'')\,\pi_v = -0.028$
$G(e')\,\pi_h = 0.148$	$G(e'')\,\pi_h = 0.127$

by Moore (*44*). From these data, the VSIE values of Mo, Mo^+, Mo^{2+}, and Mo^{3+} were found to be 6.0, 15.6, 28.2, and 46.5 eV, respectively. For the actual calculation a charge of +0.5 was chosen. By graphical interpolation this charge leads to a Coulomb integral for the *d* orbitals of $H_d = -10.4$ eV. For the energy of the *p* electrons of sulfur, the first ionization potential of H_2S, equal to $H_p = -10.4$ eV (*45*) was used.[2] According to Moore's tables, the 3*s* orbitals of sulfur lie about 9 eV below the 3*p* orbitals, so that $H_s = -19.4$ eV.

The off-diagonal elements are approximated with the Wolfsberg–Helmholz equation

$$H_{ij} = \tfrac{1}{2}FG_{ij}(H_{ii} + H_{jj});$$

for *F* the value of 2 was chosen (*46*).

From the calculations we found the e'^* and e''^* levels to be situated at 0.3 eV and 1.9 eV above the $a_1'^*$ level, respectively. This result agrees with calculations by Anzenhofer et al. (*16*).

The *d* orbitals used in these calculations are the orbitals for neutral atoms. These functions have an appreciable amplitude in regions where the amplitude of the p_σ-functions is negative. As a consequence of the charge distribution in the actual compound, the *d* orbitals are expected to have a smaller spatial extension than the orbitals for the neutral atoms. A reduction of the spatial extension of the *d* orbitals will reduce the π overlap integral, but will enhance the σ overlap. Consequently, the contribution of π-bonding is overestimated, that of σ-bonding underestimated in calculations with neutral-atom *d* functions. Therefore, the energy distance between $a_1'^*$ and e'^* levels is expected to be larger than 0.3 eV (cf. Fig. 4 for the influence of π-bonding).

The spectrum of MoS_2 shows negligible absorption for energies smaller than 1.35 eV (*47*). Thus, the $a_1'^* - e'^*$ separation is at least 1.35 eV, which indicates indeed that the calculations given above overestimate the contribution of π-bonding. If π-bonding is completely neglected, the calculations lead to more reasonable values, the e'^* and e''^* levels lie at 1.3 and 2.5 eV, respectively, above the $a_1'^*$ level. Figure 4 shows that moderate π-bonding has little influence on these values.

In the calculations we have not considered the *s* and *p* orbitals of the metal. These orbitals have a large influence on the bonding levels, but only a minor, indirect effect on the antibonding *d* levels, so that the effect of these orbitals on the ligand-field splitting is expected to be small (*48*).

Thus, semiempirical calculations for MoS_2 show that the $a_1'^*$ level is the lowest *d* level. A calculation taking into account σ-bonding only, leads to reasonable values for the ligand-field splitting; moderate π-bonding modifies these results only slightly. This indicates that the qualitative considerations of the previous section are fairly realistic for compounds of this type.

Electron Repulsion and Spin-Orbit Coupling

In this section we discuss first the effects of electron–electron repulsion for a metal atom with a d^2 configuration in trigonal-prismatic coordination (*49*). The strong-field configurations with the lowest energies are $(a_1'^*)^2$ (i.e., two electrons in the $a_1'^*$ orbital), $(a_1'^*)^1(e'^*)^1$ and $(e'^*)^2$; the ligand-field energies are 0, δ, and 2δ, respectively, if δ represents the separation between the one-electron e'^* and $a_1'^*$ levels. The electron-repulsion energies of the various terms can be expressed in terms of the Racah parameters *A*, *B*, and *C*. The total term energies are given in Table V; in Fig. 5 the reduced energies $(E - A)/B$ are plotted as a function of δ/B (the ratio C/B was taken equal to 4). The results show that for $\delta/B > 24$, the diamagnetic $^1A_1'$ term is the ground state for the d^2 ion.[3]

For the free Mo^{4+} ion the Racah parameter *B* is 0.08 eV (*50*). From general trends of the nephelauxetic ratio β_{55} in octahedral complexes (*51*), we estimate the parameter *B* for the $a_1'^*$ level of Mo^{4+} in MoS_2 to be of the order of 0.04–0.05 eV. This is consistent with our previous assumption of an effective charge of +0.5 for the metal atoms in MoS_2; if this charge is substituted in an empirical relation (*51*), which gives *B* as a function of the electron configuration and the effective charge, we

[2] This choice is analogous to taking the first ionization potential of H_2O for calculations on oxides (*43*).

[3] For small values of δ/B the two $^1A_1'$ terms will mix, but this is of little concern for our problem.

TABLE V

STRONG-FIELD TERM ENERGIES FOR A d^2 ION IN TRIGONAL-PRISMATIC COORDINATION

Strong-field configuration	Term	Energy
$(a_1'^*)^2$	$^1A_1'$	$A+4B+3C$
$(a_1'^* e'^*)$	$^3E'$	$A-8B+\delta$
	$^1E'$	$A-4B+C+\delta$
$(e'^*)^2$	$^1A_1'$	$A+4B+2C+2\delta$
	$^3A_2'$	$A+4B+2\delta$
	$^1E'$	$A+4B+2C+2\delta$

find $B = 0.046$ eV. Since δ in MoS_2 is at least 1.35 eV, we find $\delta/B \geqslant 30$. Therefore, one expects MoS_2 to have a diamagnetic ground state $^1A_1'$, in agreement with observation.

For ions with configuration $3d^2$, however, the Racah parameter B is much larger, while δ is smaller than for $4d$ or $5d$ elements. Therefore, δ/B will be smaller than the critical value of 24, and a paramagnetic ground state $^3E'$ is expected for $3d^2$ ions in a trigonal prism. It will be shown below, however, that in such cases (distorted) octahedral coordination is expected to be more favourable.

The spin-orbit splitting of the d levels in trigonal-prismatic coordination is shown in Fig. 6; the degenerate levels e'^* and e''^* are split by 2ξ and ξ,

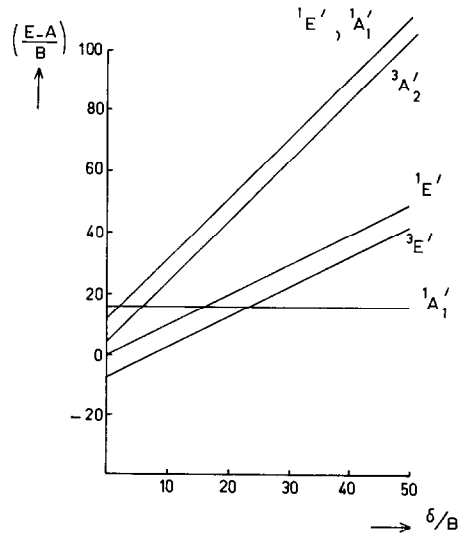

FIG. 5. Energy of strong-field terms for a d^2 ion in trigonal-prismatic coordination (for $C/B = 4$).[3]

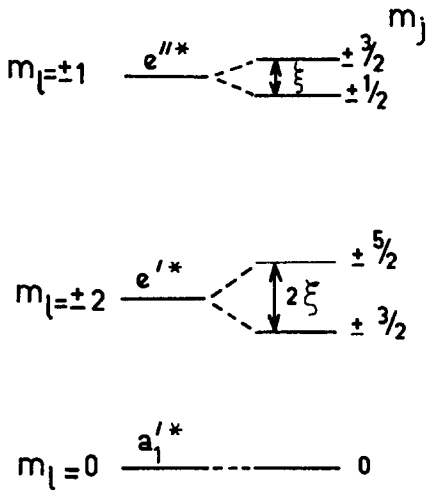

FIG. 6. Spin-orbit splitting of d levels in trigonal-prismatic coordination.

respectively. The one-electron spin-orbit coupling parameter ξ is not known very accurately for $4d$ and $5d$ elements; for Mo^{4+} and W^{4+} ions values of 0.106 and 0.28 eV have been reported (*50*, *52*). In actual compounds these values will be different as a result of covalency.

Stability of Trigonal-Prismatic Coordination

In this section an attempt is made to explain the stability of the trigonal-prismatic coordination. The discussion is based on the qualitative molecular-orbital calculations given above. A preliminary remark, however, is necessary. It is well known that reliable values for the total energy cannot be obtained from simple molecular-orbital calculations. This is because in such a one-electron model the electron–electron interactions are not properly taken into account. Thus, a summation of the energies of occupied one-electron energy levels is of little significance for the total energy. This is, however, not necessarily so for energy differences. For a comparison of a trigonal prism and an octahedron, one expects that most of the electron-repulsion energies will be very similar in the two systems. The most important difference will be due to a different anion–anion repulsion; this energy favours the octahedral coordination.

For atoms with a d^0 configuration, only the bonding and nonbonding levels are occupied. The contribution of d covalency to the energy difference $(E_p - E_0)_{cov}$ between an ideal trigonal prism ($\cos^2\theta_0 = \frac{3}{7}$) and an ideal octahedron ($\cos^2\theta_0 = \frac{1}{3}$)

for a d^0 central atom is easily calculated from the data of Tables II and III. The result is

$$(E_p - E_0)_{cov} - \Delta\left\{3 + 2(1 + 12\beta)^{1/2} - \left[1 + \left(\frac{24\beta}{49}\right)\right]^{1/2} - 2\left[1 + \left(\frac{144\beta}{49}\right)\right]^{1/2} - 2\left[1 + \left(\frac{432\beta}{49}\right)\right]^{1/2}\right\} \quad (8)$$

with $\beta = (V_\sigma/\Delta)^2$, if the same values of V_σ and Δ are used for the two systems.

There is experimental evidence that the metal–ligand distance is approximately the same for the two types of coordination. Brown and Beerntsen (*53*) determined Ta–Se distances in different polymorphs of $TaSe_2$, and obtained values of 2.59–2.60 Å for trigonal-prismatic coordination, and 2.58 Å for octahedral coordination of Ta. In β-ThI_2 (*8*) half of the metal atoms have six iodine neighbours at a distance of 3.22 Å arranged in an octahedron, while the other half of the metal atoms have six iodines at 3.20 Å in a trigonal prism. These data suggest that the assumption of equal parameters V_σ and Δ for the two types of coordination is reasonable.

In Fig. 7, $(E_p - E_0)_{cov}$ is plotted as a function of the parameter (V_σ/Δ), which is a measure of d-covalency. Since $(E_p - E_0)_{cov}$ is negative, the d-covalency stabilizes trigonal-prismatic coordination with respect to octahedral coordination.

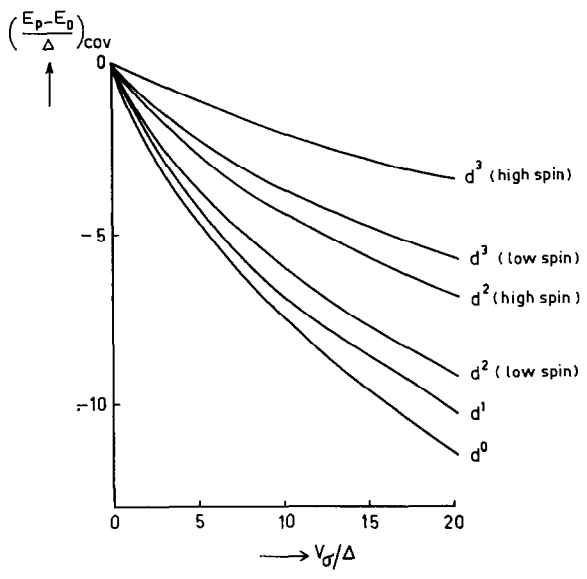

FIG. 7. The contribution of d-covalency to the energy difference between trigonal-prismatic and octahedral coordination of the central atom, as a function of the covalency parameter V_σ/Δ.[4]

The contribution of electrostatic interactions between the ions to the energy difference $E_p - E_0$ is positive, i.e., the Madelung energy favours octahedral coordination (*33*). In ionic compounds the contribution of the Madelung energy will dominate, and octahedral coordination is expected. In strongly covalent compounds the contribution of d covalency may stabilize the trigonal-prismatic coordination.

Several examples of d^0 anions in trigonal-prismatic coordination have been given in the introduction of this paper. The stabilization of the trigonal prism by increased covalency is well-illustrated by the following manganese monochalcogenides: MnS has a NaCl-type structure; MnSe has the NiAs type up to −13°C and the NaCl type at higher temperatures; while in MnTe the NiAs type is stable up to 1050°C. Examples of d^0 cations of the alkali metals in trigonal-prismatic coordination have also been given. The preference for trigonal-prismatic rather than octahedral coordination increases with increasing atomic number of both the alkali metal (d level easier accessible, i.e., smaller value of Δ) and the chalcogen ligand (more covalent bonding), as is to be expected.

The energy difference $(E_p - E_0)_{cov}$ for ions with configurations d^n $(n = 1,2,3,\ldots)$ can also be calculated from the data given in Tables II and III (see Fig. 7). For d^2 and d^3 ions in a trigonal prism both the low-spin and the high-spin configurations are compared with the high-spin configuration in an octahedron.[4]

Taking into account that the Madelung energy favours octahedral coordination, it is seen from Fig. 7 that trigonal-prismatic coordination is most likely in predominantly covalent compounds of ions with configurations d^0, d^1, and low-spin d^2; it is less likely for ions with high-spin d^2 and low-spin d^3 configurations, and it is not expected for high-spin d^3 ions and ions with more than three d electrons.

The transition metals in trigonal-prismatic coordination given in examples (1) and (5) of the introduction nearly all have configurations d^1 or low-spin d^2. In the intercalation compounds M_pNbX_2 and M_pTaX_2 (M = Nb, Ta, Cu, Ag, 3d-transition metal, alkali metal; X = S, Se) of examples (3) and (4), the electron configuration of

[4] The effect of electron repulsion is neglected in Fig. 7. This effect decreases the stabilization of the prismatic coordination of low-spin d^2 and d^3 ions; the corrected stabilization will lie between the curves for the low-spin and high-spin configurations given in the figure.

Nb, Ta is between d^1 and d^2, and the coordination is trigonal-prismatic. In the corresponding compounds of Mo and W the configuration would be between d^2 and d^3; these compounds are unknown, except for the very unstable intercalation compounds of the alkali metals and for $CoMo_2S_4$ where Mo has a distorted octahedral coordination (*54*).

In the following we shall discuss the dichalcogenides of Nb and Ta (d^1) and of Mo and W (d^2) in some more detail; we remark that the d^3 metal atoms in ReS_2 (*47*) and $ReSe_2$ (*55*) have (strongly distorted) octahedral coordination.

Physical Properties of the Dichalcogenides of Nb, Ta, Mo, and W

The magnetic, electrical and optical properties of the dichalcogenides of Nb, Ta, Mo, and W have been studied in considerable detail (*37*). The disulfides and diselenides of Mo and W are diamagnetic semiconductors, whereas the disulfides and diselenides of Nb and Ta are metallic and pauliparamagnetic. $MoTe_2$ undergoes at about 850°C a phase transition from a semiconducting α-phase with trigonal-prismatic coordination to a metallic β-phase in which the metal atoms have a distorted octahedral coordination (*31*). These data show that the electrical properties of these compounds depend on the number of *d*-electrons and on the coordination of the metal atoms. In this section we shall try to interpret the gross physical properties in terms of schematic energy-band models.

The physical properties of transition-metal compounds depend to a large extent on the ligand-field splitting of the metal *d* orbitals. In solids the *d* levels broaden into narrow energy bands, which, if partly occupied, lead to metallic conductivity by *d* electrons. Other electronic states, derived from the outer *s* and *p* orbitals of metal and ligand atoms, should also be considered. These states give rise to broad energy bands: a valence band consisting mainly of *s* and *p* orbitals of the anions (bonding states), and a conduction band (mainly *s* and *p* orbitals of the metal, antibonding states).

From molecular-orbital calculations we expect that the nondegenerate $a_1'^*$ level has the lowest energy of the *d* levels in trigonal-prismatic coordination. The physical properties also favour this conclusion. For the dichalcogenides of Mo and W, therefore, a diamagnetic $(a_1'^*)^2 - {}^1A_1'$ ground state is expected, leading to diamagnetic semiconductors, as is observed.

Goodenough (*35*) proposed a ligand-field splitting for trigonal-prismatic coordination with e'^* as the lowest *d* level. For atoms with d^2 configuration, this would lead to metallic conductivity, as a result of the partial filling of the e'^* band. In order to explain the semiconducting properties of the disulfides and diselenides of Mo and W, Goodenough takes into account the spin-orbit splitting of the e'^* band. The two *d* electrons would occupy the $m_j = \pm\frac{3}{2}$ level. This model leads to a semiconductor; however, the energy gap would correspond to the energy difference between the $m_j = \pm\frac{3}{2}$ and $m_j = \pm\frac{5}{2}$ levels derived from e'^*. The observed optical band gap of MoS_2 is about 1.35 eV (*47*), which is much larger than the expected spin-orbit splitting of the e'^* level.

According to Wilson and Yoffe (*37*), the $a_1'^* - e'^*$ energy difference (in their nomenclature: d_z^2 and *d*/*p* bands) in MoS_2 is about 0.2 eV. They report a weak infrared absorption edge at 0.2 eV, with absorption coefficients $\alpha \approx 200$ cm^{-1}. However, $a_1'^* - e'^*$ transitions are allowed electric dipole transitions, and are expected to have an appreciable oscillator strength, leading to much higher values of α. Moreover, in recent experiments (*47*) no absorption edge at 0.2 eV could be detected in MoS_2. Therefore, in our opinion, the semiconducting and optical properties of MoS_2 and similar compounds are consistent only with an energy-level scheme with the e'^* and e''^* levels at more than 1 eV above the doubly occupied $a_1'^*$ level.

In the dichalcogenides of Nb and Ta, the metal atoms have a d^1 configuration, leading to a partly filled narrow $a_1'^*$ band. This explains the metallic conductivity of these compounds.

For a distorted octahedral coordination, as is found in β-$MoTe_2$ and WTe_2 (symmetry approximately C_{3v}), the lowest *d* level is a degenerate e^* level (*49*); the metallic conductivity is a consequence of this partly occupied e^* band (*31*).

For a discussion of the physical properties of the transition-metal dichalcogenides, the position of the narrow *d* bands with respect to the broad valence and conduction bands should be considered (*56*, *57*). Data, to be presented below, indicate an overlap of the valence band with the $a_1'^*$ band, and an overlap of the conduction band with the e'^* band in the dichalcogenides of Nb, Ta, Mo, and W with trigonal-prismatic coordination of the metal. This leads to energy-band diagrams of the type shown in Fig. 8.

Data on Hall and Seebeck effects of $TaSe_2$ and $NbSe_2$ indicate a mixed type of conduction, i.e., by electrons and holes (*58*, *59*). Similar conclusions were obtained from studies of the transport properties of NbS_2 and TaS_2 (*60*, *61*). This indicates that

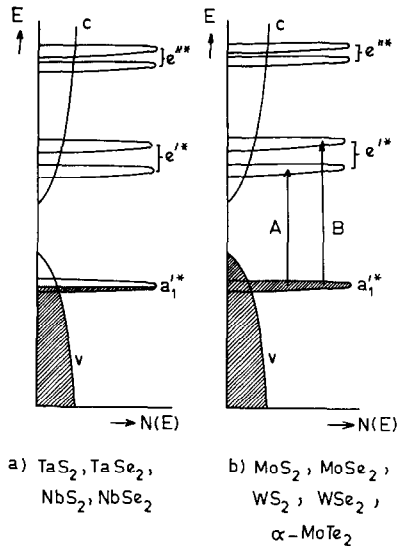

FIG. 8. Schematic energy-band diagrams for the dichalcogenides of Nb, Ta, Mo, and W with trigonal-prismatic coordination of the metal. The energy E of the electronic states is plotted as a function of the density of states $N(E)$. States occupied by electrons are hatched; V = valence band, C = conduction band.

in these compounds the valence band overlaps the narrow $a_1'^*$ band, in accordance with an energy-band diagram as drawn in Fig. 8(a).

The mobility of holes in p-type MoS_2 is of the order of 100 $cm^2/V\cdot sec$ (*37*) at room temperature; similar values are obtained for the mobility of holes in nontransition-metal compounds such as ZnS (*62*). In the latter compounds the holes occupy states of a broad valence band. If p-type conduction in MoS_2 were due to holes in a narrow $a_1'^*$ band, the mobility would presumably be much lower. Thus, the high mobility of holes in p-type MoS_2 indicates that the top of the valence band lies above the narrow $a_1'^*$ band.

In a similar way the high mobility of electrons in n-type MoS_2 (*37*) indicates that the electrons occupy states in the broad conduction band, and therefore, that the bottom of the conduction band lies below the e'^* and e''^* narrow bands.[5] From data on the Seebeck effect (*37*) one can estimate the effective mass of the electrons; the result $m^* \approx m_0$ again indicates conduction by broad-band electrons.

[5] In magnetic semiconductors, charge carriers in a broad energy band may have a low mobility (of the order of 1 $cm^2/V\cdot sec$) as a result of spin-disorder scattering (*57*). However, this scattering mechanism is not present in diamagnetic semiconductors. Therefore, one expects high mobilities of broad-band charge carriers in diamagnetic semiconductors.

Thus, for MoS_2, the energy-band diagram is presumably of the type sketched in Fig. 8(b). In the selenides and tellurides the gap between valence and conduction band is expected to be smaller, as a consequence of the smaller electronegativity of the anions; this makes an overlap of the valence band with the $a_1'^*$ band, and of the conduction band with the e'^* and e''^* bands even more probable. Moreover, the large values of the mobilities, observed in n- and p-type WSe_2 (*63*), also indicate conduction by charge carriers in broad bands.

Absorption spectra of the dichalcogenides of Mo and W show an absorption edge at about 1 eV, and at least two strong absorption peaks A and B at higher energies (*37*). We propose that the edge absorption in MoS_2 at 1.35 eV (*47*) is due to transitions from the valence band to the conduction band, and that the absorption peaks A and B are due to transitions from the $a_1'^*$ band to the two levels $m_j = \frac{3}{2}$ and $m_j = \frac{5}{2}$ of the e'^* band. One-electron electric dipole transitions from $a_1'^*$ to e'^* are allowed for light polarized perpendicular to the trigonal axis. The transition probability for such transitions is expected to be appreciable, as a result of the strong covalency and the absence of an inversion center. Indeed, the observed oscillator strength of the peaks A and B [$f \approx 5 \times 10^{-3}$ (*37*)] is comparable with the oscillator strength of spin-allowed ligand-field transitions in tetrahedral complexes [e.g., $CoCl_4^{2-}$, $f \approx 5 \times 10^{-3}$ (*50*)].

As the splitting of the $a_1'^*$ to e'^* transition into two peaks A and B is attributed to spin-orbit splitting of the e'^* band, one expects the oscillator strengths of the two peaks to be equal, as is indeed observed (*37*). From the spin-orbit coupling parameters of free Mo^{4+} and W^{4+} ions one calculates splittings of 0.212 and 0.56 eV, respectively. These values are compatible with the observed A–B splittings of 0.20 eV (MoS_2) and 0.37 eV (WS_2) (*37*). In the selenides and tellurides the A–B splittings are larger (*37*); we attribute this to a contribution of the spin-orbit coupling of the ligand p-orbitals. The strong covalency of selenides and tellurides leads to a strong mixing of d-orbitals with anion p-orbitals. The spin-orbit coupling of p-orbitals of Se and Te is quite large—$\xi_{4p,Se} = 0.28$ eV; $\xi_{5p,Te} = 0.56$ eV (*52*). Therefore, d–p mixing might result in an appreciable increase of the spin-orbit splitting of the e'^* band.

Acknowledgments

We are grateful to Drs. A. J. H. Wachters, Drs. D. Kracht, and Prof. W. C. Nieuwpoort of the Department of Theoretical

Chemistry for valuable discussions and help with the calculations. This investigation was supported by the Netherlands Foundation for Chemical Research (SON) with financial aid from the Netherlands Organization for the Advancement of Pure Research (ZWO).

References

1. A. E. Smith, G. N. Schrauzer, V. P. Mayweg, and W. Heinrich, *J. Amer. Chem. Soc.* **87**, 5798 (1965).
2. R. Eisenberg and J. A. Ibers, *Inorg. Chem.* **5**, 411 (1966).
3. R. Eisenberg, E. I. Stiefel, R. C. Rosenberg, and H. B. Gray, *J. Amer. Chem. Soc.* **88**, 2874 (1966).
4. E. I. Stiefel, R. Eisenberg, R. C. Rosenberg, and H. B. Gray, *J. Amer. Chem. Soc.* **88**, 2956 (1966).
5. G. N. Schrauzer and V. P. Mayweg, *J. Amer. Chem. Soc.* **88**, 3235 (1966).
6. F. Jellinek, *Ark. Kemi* **20**, 447 (1963).
7. F. Hulliger, *Struct. Bonding, Berlin* **4**, 83 (1968).
8. L. J. Guggenberger and R. A. Jacobson, *Inorg. Chem.* **7**, 2257 (1968).
9. R. Huisman, F. Kadijk, and F. Jellinek, *J. Less Common Metals* **21**, 187 (1970).
10. K. Koerts, *Acta Crystallogr.* **16**, 432 (1963).
11. J. M. van den Berg and C. W. F. Kort, *J. Less Common Metals* **13**, 363 (1967).
12. J. M. van den Berg and P. Cossee, *Inorg. Chim. Acta* **2**, 143 (1968).
13. B. van Laar, H. M. Rietveld, and D. J. W. Ijdo, *in* "Third Int. Conf. Solid Compounds Transition Elements," Oslo, 1969.
14. F. Hulliger and E. Pobitschka, *J. Solid State Chem.* **1**, 117 (1970).
15. J. M. Voorhoeve-van den Berg and M. Robbins, *J. Solid State Chem.* **1**, 134 (1970).
16. K. Anzenhofer, J. M. van den Berg, P. Cossee, and J. N. Helle, *J. Phys. Chem. Solids* **31**, 1057 (1970).
17. W. Rüdorff, *Chimia* **19**, 489 (1965).
18. W. P. F. A. M. Omloo and F. Jellinek, *J. Less Common Metals* **20**, 121 (1970).
19. G. Grams, Dissertation, Tübingen, 1961.
20. M. Danot, A. Le Blanc, and J. Rouxel, *Bull. Soc. Chim. Fr* **1969**, 2670 (1969).
21. M. Rüdorff, A. Stössel, and V. Schmidt, *Z. Anorg. Allg. Chem.* **357**, 264 (1968).
22. S. Rundqvist and T. Lundström, *Acta Chem. Scand.* **17**, 37 (1963).
23. H. Hahn and P. Ness, *Z. Anorg. Allg. Chem.* **302**, 37, 136 (1959).
24. H. F. Franzen and J. Graham, *J. Inorg. Nucl. Chem.* **28**, 377 (1966).
25. H. F. Franzen, private communication.
26. F. Jellinek, *Oesterr. Chem. Zt.* **60**, 311 (1959).
27. A. F. Andresen and H. Røtterud, *in* "Third Int. Conf. Solid Compounds Transition Elements," Oslo, 1969.
28. W. D. Johnston and D. E. Sestrick, *J. Inorg. Nucl. Chem.* **19**, 229 (1961).
29. R. Huisman and F. Jellinek, *J. Less Common Metals* **17**, 111 (1969).
30. F. Kadijk, Dissertation, Groningen, 1969.
31. M. B. Vellinga, R. de Jonge, and C. Haas, *J. Solid State Chem.*, **2**, 299 (1970).
32. R. Huisman, Dissertation, Groningen, 1969.
33. R. J. de Munk, "Afstudeerverslag," Delft, 1967.
34. K. Koerts, Dissertation, Leiden, 1964.
35. J. B. Goodenough, *Mater. Res. Bull.* **3**, 409 (1968).
36. R. Huisman, R. de Jonge, and C. Haas, *in* "Third Int. Conf. Solid Compounds Transition Elements," Oslo, 1969.
37. J. A. Wilson and A. D. Yoffe, *Advan. Phys.* **18**, 193 (1969).
38. J. S. Griffith, "The Theory of Transition Metal Ions," Cambridge University Press, London, 1961.
39. J. C. Slater, *Phys. Rev.* **36**, 57 (1930).
40. H. Basch and H. B. Gray, *Theor. Chim. Acta* **4**, 367 (1966).
41. E. Clementi, *J. Chem. Phys.* **40**, 1944 (1964); IBM Technical Report RJ-256, August 1966.
42. C. J. Ballhausen and H. B. Gray, "Molecular Orbital Theory," W. A. Benjamin Inc., New York, 1964.
43. A. Viste and H. B. Gray, *Inorg. Chem.* **3**, 1113 (1964).
44. C. E. Moore, *Nat. Bur. Stand. U.S. Circ.* **467**, vol. II (1952).
45. W. C. Price, *J. Chem. Phys.* **4**, 147 (1936).
46. M. Wolfsberg and L. Helmholz, *J. Chem. Phys.* **20**, 837 (1952).
47. J. C. Wildervanck, Dissertation, Groningen, 1970.
48. F. L. M. A. H. de Laat, Dissertation, Eindhoven, 1968.
49. R. de Jonge, Dissertation, Groningen, 1970.
50. B. N. Figgis, "Introduction to Ligand Fields," Interscience Publ., New York, 1966.
51. C. K. Jørgensen, "Oxidation Numbers and Oxidation States," Chap. 5, Springer-Verlag, Berlin/New York, 1969.
52. F. Herman and S. Skillmann, "Atomic Structure Calculations," Prentice-Hall Inc., Englewood Cliffs, N. J., 1963.
53. B. E. Brown and D. J. Beerntsen, *Acta Crystallogr.* **18**, 31 (1965).
54. J. M. van den Berg, *Inorg. Chim. Acta* **2**, 216 (1968).
55. N. W. Alcock and A. Kjekshus, *Acta Chem. Scand.* **19**, 79 (1965).
56. W. Albers and C. Haas, *Phys. Lett.* **8**, 300 (1964).
57. C. Haas, *Crit. Rev. Solid State Sci.* **1**, 49 (1970).
58. H. N. S. Lee, H. McKinzie, D. S. Tannhauser, and A. Wold, *J. Appl. Phys.* **40**, 602 (1969).
59. H. N. S. Lee, M. Garcia, H. McKinzie, and A. Wold, *J. Solid State Chem.* **1**, 190 (1969).
60. M. H. van Maaren and H. B. Harland, *in* "Third Int. Conf. Solid Compounds Transition Elements," Oslo, 1969.
61. M. H. van Maaren and H. B. Harland, *Phys. Lett. A* **29**, 571 (1969).
62. B. Ray, "II–VI Compounds," Pergamon Press, London, 1969.
63. L. C. Upadhyayula, J. J. Loferski, A. Wold, W. Giriat, and R. Kershaw, *J. Appl. Phys.* **39**, 4736 (1968).